References

[1] Zelazny, S. W., Driscoll, R. J., Raymonda, J. W., Blauer, J. H., and Soloman, W. C., "Modeling DF/HF Lasers: An Examination of Key Assumptions," *AIAA Journal*, Vol. 16, March 1978, p. 297.

[2] Roshko, A., "Structure of Turbulent Shear Flows: A New Look," *AIAA Journal*, Vol. 14, 1976, p. 1349.

[3] Murthy, S.N.B., (ed.), *Turbulent Mixing in Non-Reactive and Reactive Flows*, Plenum Press, New York, 1975.

[4] Waypa, J., Engle, J. W., and Wilson, L. E., "The Schlieren System as a Chemical Laser Optical Cavity Diagnostic," Air Force Weapons Laboratory, Kritland Air Force Base, N. Mex., AFWL-TR-73, 1973, p. 273.

[5] Cummings, J. C., Aeschliman, O. P., and Mulac, A. J., "Raman Spectroscopy in a CW Chemical Laser," *Journal of Quantitative Spectroscopy and Radiative Transfer*, Vol. 19, 1978, p. 493.

[6] Maya, F., Druet, S., Pealot, M., and Taran, J. P., "Flame Investigation by Coherent Anti-Stokes Raman Scattering," AIAA Paper 76-29, Washington, D.C., 1976.

[7] Hackett, C. E., "Laser Velocimetry Measurements in the Cavity of HF Chemical Laser (Cavity Injector Type CL-11)," Sandia Laboratories, Rept. SAND 76-9314, 1977.

[8] Morris, P. J., "Turbulence Measurements in Subsonic and Supersonic Axis Symmetric Jets in a Parallel Stream," *AIAA Journal*, Vol. 14, Oct. 1976, p. 1468.

[9] Bershader, D., Prakask, S. G., and Huker, G., "Improved Flow Visualization by Use of Resonant Refractivity," *Progress in Astronautics and Aeronautics, Experimental Diagnostics in Gas Phase Combustion Systems*, Vol. 53, edited by B. T. Zinn, 1977, p. 595.

[10] Daily, J. W. and Chan, C., "Laser Induced Fluorescence Measurement of Sodium in Flames," *Sixth International Colloquium on Gasdynamics of Explosions and Reactive Systems*, Stockholm, Aug. 1977.

[11] Wrobel, N. H. and Pratt, N. H., "Laser Induced Sodium Fluorescence Measurements in a Turbulent Propane Diffusion Flame," *17th International Symposium on Combustion*, Leeds, 1978.

[12] Levy, D. H., Wharton, L., and Smalley, R. E., "Laser Spectroscopy in Supersonic Jets," *Chemical and Biochemical Applications of Lasers*, Academic Press, New York, 1977.

Transonic Shock/Boundary-Layer Interaction Subject to Large Pressure Fluctuations

S. Raghunathan* and J. B. Coll†
The Queen's University of Belfast, Northern Ireland
and
D. G. Mabey‡
Royal Aircraft Establishment, Bedford, England

Nomenclature

c	= chord length
c_p	= pressure coefficient $p - p_1/\frac{1}{2}\rho_1 U_1^2$
$c_p{}^*$	= pressure coefficient at $M=1$
f	= frequency, Hz
$F(n)$	= contribution to $\tilde{p}^2/q^2$ in frequency band Δn
$\sqrt{n(F(\ ))}$	$= p/q(\epsilon)^{1/2}$
M	= Mach number
n	= frequency parameter fw/U_1
p	= pressure
q	= freestream dynamic pressure $\frac{1}{2}\rho U_1^2$
R_θ	= momentum thickness Reynolds number $U_1\theta/\nu$
U_1	= freestream velocity
u	= local velocity
w	= tunnel width
X_s	= shock position
θ	= boundary-layer momentum thickness $= \int_0^\infty \rho u/\rho_1 U_1 (1-\rho u/\rho_1 U_1)\,\mathrm{d}y$
ϵ	= analyzer bandwidth ratio $\Delta f/f$
ν	= kinematic viscosity

Superscript

$(\tilde{\ })$	= root-mean-square value

Subscript

1	= freestream conditions

Introduction

A RECENT Note[1] showed that for attached subsonic and transonic boundary layers with small pressure gradients the turbulence within the boundary layer is influenced by the external pressure fluctuations, but that the corresponding changes in the mean properties of the boundary layer are fairly small. The influence of pressure fluctuations on a boundary layer with a shock interaction, however, is not understood. Robertson's experiments on a missile body[2] showed strong effects of pressure fluctuations on the shock/boundary-layer interaction. The shock wave oscillations were strongly correlated with the freestream pressure fluctuations. The levels of pressure fluctuations in the tunnel during the tests were within the range $\tilde{p}/q = 0.7$-1.2%. The work of Ross and Rohne[3] on a supercritical airfoil with smaller freestream noise levels ($\tilde{p}/q = 0.35$-0.6%) showed no effect of pressure fluctuations on the shock separation and trailing-edge pressure coefficient. However, even these low-noise levels changed the boundary-layer transition. This Note presents some information obtained on a transonic shock/turbulent boundary-layer interaction subject to pressure fluctuations from 0.6% to 1.5%.

Tests

The tests were made in the 101×101 mm transonic tunnel at The Queen's University of Belfast. The model was a half-double wedge-shaped airfoil of 9% thickness with an aspect ratio of 1, giving a blockage of 9.0% set on the tunnel roof. The R_θ of the turbulent boundary layer at the leading edge of the model was about 10^4. Pressure fluctuations were varied by changing the number of slots in the floor of the tunnel and partially or fully closing the slots with perforated screens without significantly changing the mean pressure distribution in the tunnel in the presence of the model.

The freestream pressure p_1 was measured two chords upstream of the model. An adjustable choke downstream of the test section was used to set any desired freestream Mach number. Measurements were made of pressure distribution on the model for several shock strengths and, for a fixed shock position, of the boundary-layer mean and turbulence velocity profiles at the trailing edge. The boundary-layer separation and reattachment points were established by the china clay technique.

Results

Figure 1 shows typical spectra at $M=0.78$ of the pressure fluctuations for the three test conditions. The peak value of $\sqrt{nF(n)}$ vary from 0.6×10^{-2} to 1.8×10^{-2}. These values of $\sqrt{nF(n)}$ are, respectively, typical of pressure fluctuation levels that exist in rather noisy and very noisy ventilated

Received April 27, 1979.

Index categories: Boundary Layers and Convective Heat Transfer—Turbulent; Subsonic Flow; Transonic Flow.

*Lecturer, Department, of Aeronautical Engineering.
†Research Assistant. Member AIAA.
‡Principal Scientific Officer, Structures Department.

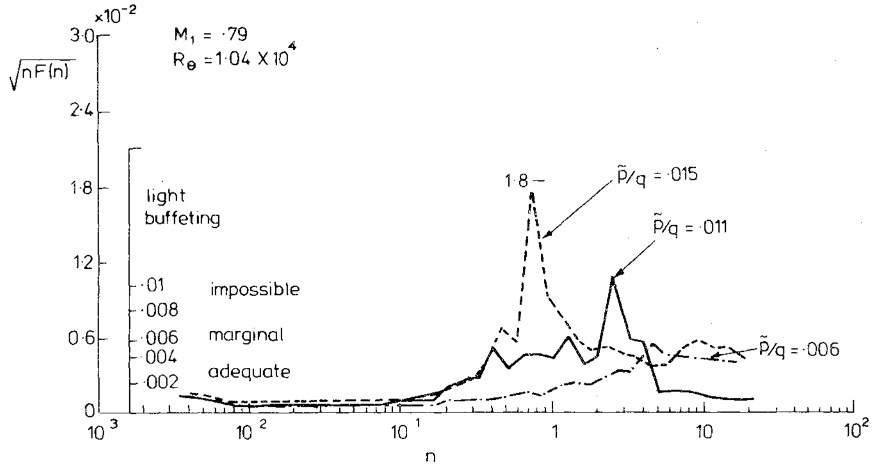

Fig. 1 Spectra of pressure fluctuations.

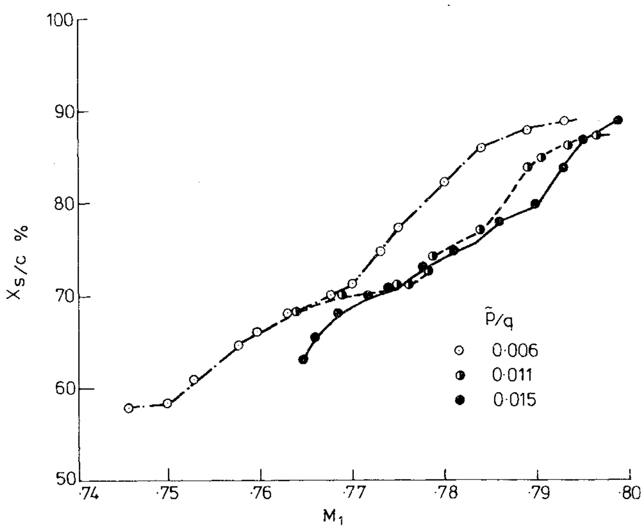

Fig. 2 Influence of pressure fluctuations on shock position.

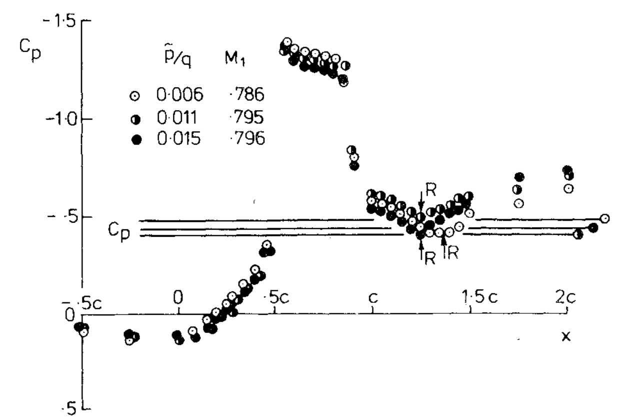

Fig. 3 Influence of pressure fluctuations on the pressure distribution.

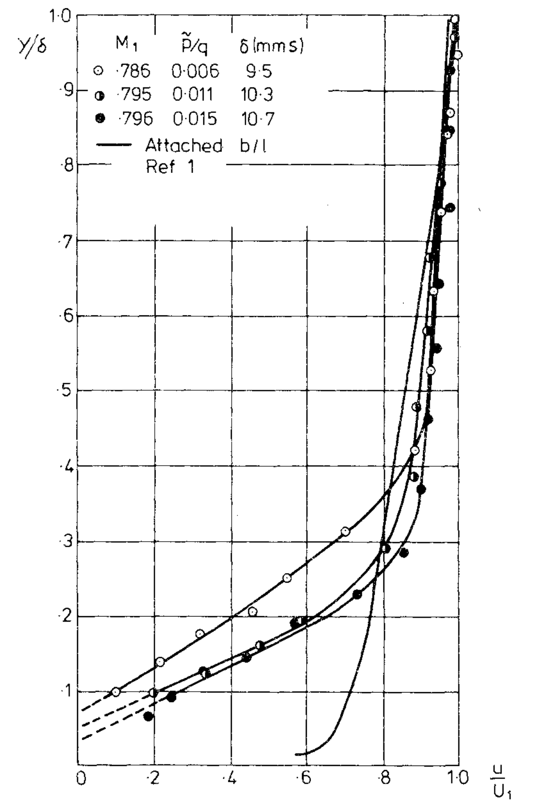

Fig. 4 Velocity profiles at the trailing edge.

tunnels, as may be seen by comparison with the criteria for levels of flow unsteadiness for buffeting tests proposed by Mabey.[4]

Flow patterns obtained by the china clay technique revealed two-dimensional flow in the middle of the model covering more than half the span. For a given shock position, the three-dimensional flow pattern at the junction between the model and the side walls of the tunnel was invariant with the changes in the pressure fluctuation levels.

The variation of shock position with the freestream Mach number for the three levels of pressure fluctuations is shown in Fig. 2. There is a substantial change in the shock position when the fluctuations increase from $\tilde{p}/q$ = 0.006 to .0011, the shock moving upstream with the increase in pressure fluctuations. There is no further marked change in the shock position when fluctuation levels increase from $\tilde{p}/q$ = .011-.015.

Figure 3 shows the pressure distributions on the model for a fixed shock position of $x_s/c_l = 0.87$ and for the three levels of pressure fluctuations. The shock/boundary-layer interaction involves complete boundary-layer separation with the reattachment downstream of the model. There is a strong influence of pressure fluctuations on the trailing edge C_p. The reattachment point, as observed from the pressure distribution $C_{p_{max}}$ and verified by the china clay technique, changes with the increase in $\tilde{p}/q$ up to a level of $\tilde{p}/q$ = .011, beyond which the change is insignificant.

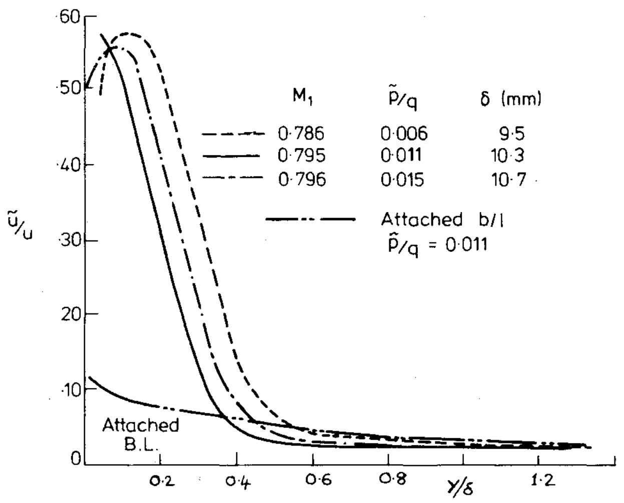

Fig. 5 Turbulence profiles at the trailing edge.

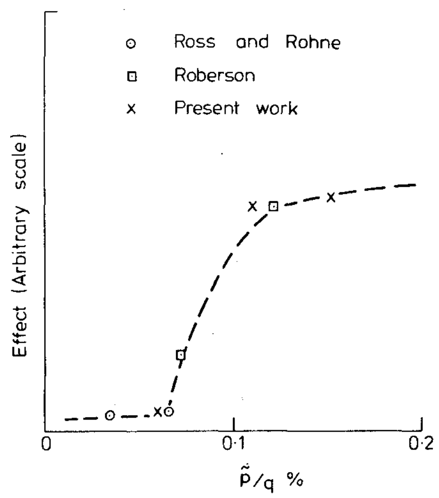

Fig. 6 A model for the effect of pressure fluctuations.

The boundary-layer velocity profiles at the trailing edge of the model for the three levels of pressure fluctuations are shown in Fig. 4. There is a considerable change in the velocity profiles when the levels of $\tilde{p}/q$ were changed from .006 to .011. The changes, with further increases in $\tilde{p}/q$, are not noticeable.

Figure 5 shows the turbulence profiles at the trailing edge for the three levels of $\tilde{p}/q$. A typical turbulence profile obtained in an attached turbulent boundary layer at zero pressure gradient[1] is also shown for comparison. The levels of turbulence in the separated layer are generally an order higher than those in an attached boundary layer. The levels are sensitive to the changes in $\tilde{p}/q$. With the increase in pressure fluctuation levels, the turbulence initially increases and then decreases. However, the changes in the freestream turbulence levels are insignificant for all levels of $\tilde{p}/q$ remaining constant at about 2.4%

The general effect of pressure fluctuations on the shock/boundary-layer interaction is shown schematically in Fig. 6. It is suggested that there is virtually no effect of pressure fluctuations up to a level of about 0.6%. With the increase in pressure fluctuations, whether the effect beyond this level is gradual or sudden is uncertain and needs further investigation.

Acknowledgment

This work originated as part of the research supported by S.R.C. Contract B/RG/8932 and GR/A/53772.

References

[1] Raghunathan, S., Coll, J. B., and Mabey, D. G., "Flat Plate Turbulent Boundary Layers Subject to Large Pressure Fluctuations," *AIAA Journal*, to be published.

[2] Robertson, J. M., "Unsteady Pressure Phenomena for Basic Missile Shapes at Transonic Speeds," AIAA Paper 64-3, 1974.

[3] Ross, R. and Rohne, P. B., "The Character of Flow Unsteadiness and Its Influence on Steady State Transonic Wind Tunnel Measurements," AGARD CP-174, Paper 45.

[4] Mabey, D. G., "Flow Unsteadiness of Mode Vibration in Wind Tunnels at Subsonic or Transonic Speeds," ARC CP 1155, 1971.

Radiation Shape Factors between End Plane and Outer Wall of Concentric Tubular Enclosures

C. P. Minning*
Hughes Aircraft Company, Culver City, Calif.

Nomenclature

x,y,z	= Cartesian coordinates of dA_1, cm
l_1,m_1,n_1	= cosines (i.e., direction cosines) of the angles between the normal to dA_1 and the x, y, and z axes, respectively
x_2,y_2,z_2	= Cartesian coordinates of a point on the periphery of surface 2, cm
S	= distance between dA_1 and a point on the periphery of surface 2, cm
r	= radial coordinate in plane of dA_1, cm
r_o	= radius of outer tube, cm
r_i	= radius of inner tube, cm
θ	= angular displacement from x axis, rad
ω	= view angle, rad
h	= height of concentric tubes, cm

Introduction

In radiation heat-transfer calculations for diverse applications such as gas turbine combustion chambers, rotary-kiln dryers, and spin-stabilized spacecraft, it is often desired to calculate the shape factor between an annular-disk end plane and the outer wall of an enclosure formed by concentric cylinders, such as that shown in Fig. 1. If the inner and outer radii of the disk are the same as the radii of the inner and outer cylinders, the shape factor can be calculated by means of the closed-form expressions given in Ref. 2. However, there is no closed-form expression available in the literature for the case where the radii of the annular disk are not equal to the radii of the concentric cylinders.

The contour integral method is used in the present analysis to derive a closed-form expression for the shape factor, $F_{dA_1\text{-}A_2}$, from a differential area on the annular-disk end plane to the outer wall of the enclosure. This expression can then be integrated numerically to obtain the desired shape factor from a finite-sized annular disk to the outer wall. Typical results are shown for both configurations.

Analysis

Consider the geometry shown in Figs. 1-3 which illustrate the nomenclature used in this presentation. Throughout this

Received May 10, 1979.

Index categories: Spacecraft Temperature Control; Radiation and Radiative Heat Transfer; Thermal Modeling and Analysis.

*Senior Staff Engineer, Electro-Optical and Data Systems Group.